PAPER

First principles investigation of carbon-screw dislocation interactions in body-centered cubic metals

IOP Publishing Modelling and Simulation in Materials Science and Engineering
Modelling Simul. Mater. Sci. Eng. **25** (2017) 084001 (13pp) https://doi.org/10.1088/1361-651X/aa88eb

First principles investigation of carbon-screw dislocation interactions in body-centered cubic metals

B Lüthi[1], L Ventelon[1], C Elsässer[2,3], D Rodney[4] and F Willaime[5]

[1] DEN-Service de Recherches de Métallurgie Physique, CEA, Université Paris-Saclay, F-91191 Gif-sur-Yvette, France
[2] Fraunhofer Institute for Mechanics of Materials IWM, Wöhlerstr. 11, D-79108 Freiburg, Germany
[3] University of Freiburg, Freiburg Materials Research Center, Stefan-Meier-Str. 21, D-79104 Freiburg, Germany
[4] Institut Lumière Matière, CNRS-Université Claude Bernard Lyon 1, F-69622 Villeurbanne, France
[5] DEN-Département des Matériaux pour le Nucléaire, CEA, Université Paris-Saclay, F-91191 Gif-sur-Yvette, France

E-mail: lisa.ventelon@cea.fr

Received 3 April 2017, revised 24 August 2017
Accepted for publication 29 August 2017
Published 6 October 2017

Abstract

Using *ab initio* density functional theory calculations, we investigate the effect of interstitial carbon solutes on $1/2\langle 111\rangle$ screw dislocations in non-magnetic body-centered cubic transition metals from group 5 (V, Nb, Ta) and group 6 (Mo, W). The two groups are found to display different solute–dislocation interaction behaviors. Group 6 shows a core reconstruction similar to that previously reported in Fe(C): the dislocation adopts a hard-core configuration with the carbon atoms at the center of regular trigonal prisms formed by the metal atoms. The solute–dislocation interaction energies are strongly attractive, ranging from -1.3 to -1.9 eV depending on the metal and the carbon–carbon distance. By way of contrast, the configuration of lowest energy in group 5 consists of the dislocation in its easy core and the carbon atom in a fifth nearest neighbor octahedral site. The configuration is attractive, but less than in group 6. We show that this group dependence is consistent with the carbon local environment in the stable stoichiometric carbide structures, namely cubic NaCl-type for group 5 and hexagonal WC-type for group 6: in both cases the carbon atoms are at the center of octahedra and prisms respectively.

Keywords: DFT calculations, dislocation–solute interaction, BCC transition metals

(Some figures may appear in colour only in the online journal)

1. Introduction

The mechanical properties of metals are deeply modified by the presence of solute atoms, because for instance of the formation of Cottrell atmospheres around dislocation lines (Cottrell and Bilby 1949) or the precipitation of carbides that are much harder than their parent metals (Goldschmidt 1967, Toth 1971, Oyama 1996). Several authors have used elasticity theory and interatomic potential calculations to study the interactions between dislocations and solute atoms. In the case of body-centered cubic (BCC) metals of particular interest here, recent works include (Tapasa *et al* 2007, Clouet *et al* 2009, Ishii *et al* 2013, Chockalingam *et al* 2014, Veiga *et al* 2015). However, only a few have used density functional theory (DFT) to investigate core effects quantitatively (Trinkle and Woodward 2005, Medvedeva *et al* 2007, Romaner *et al* 2010, Zhao and Lu 2011, Li *et al* 2012, Itakura *et al* 2013, Samolyuk *et al* 2013, Romaner *et al* 2014, Rodney *et al* 2016). Recent DFT studies in BCC Fe(X) with X = B, C, N and O (Ventelon *et al* 2015, Lüthi *et al* 2016) showed that the presence of interstitial solute atoms can induce a reconstruction of the $1/2\langle 111\rangle$ screw dislocation core from its so-called easy core configuration to a hard core configuration, along with a strongly attractive interaction energy. In the present work, we assess the generality of this unexpected reconstruction using DFT in all non-magnetic BCC transition metals: V, Nb and Ta from group 5 and Mo and W from group 6. Thereafter, these systems are referred to as *M*5(C), where *M*5 = V, Nb, Ta and *M*6(C) where *M*6 = Mo, W.

The paper is organized as follows. In section 2, the methodology of the DFT calculations is described and the various interaction energies are defined. Results for two basic quantities are provided and compared to previous calculations: the solution energies of carbon atoms in octahedral and tetrahedral sites and the energy difference between easy and hard core configurations. In section 3, carbon–dislocation interactions are investigated in group 6 first and then group 5. In section 4, we discuss the present results, both in terms of the contribution of elastic strains to the stability of carbon configurations and in terms of the relative stability of bulk metal-carbide structures.

2. Methodology

The DFT calculations were carried out with the VASP code (Kresse and Furthmüller 1996) using the projector augmented wave pseudopotential scheme (Blöchl 1994, Kresse and Joubert 1999) within the Perdew–Burke–Ernzerhof generalized gradient approximation. Pseudopotentials with p-semicore electrons for V, Nb, Ta, Mo and W were used. All calculations were performed using a 400 eV kinetic-energy cutoff, a first order Hermite–Gaussian occupation scheme with a broadening of 0.2 eV and a convergence criterion on forces of 10^{-2} eV $\mathrm{\AA}^{-1}$ for structural relaxations.

A quadrupolar periodic array of dislocation dipoles was adopted for dislocation calculations (Ventelon *et al* 2013), with solute atoms separated by 1*b* or 2*b* along the $\langle 111\rangle$ direction (*b* is the dislocation Burgers vector), resulting in simulation cells with 135 or 270 metal atoms. $1 \times 2 \times 16$ and $1 \times 2 \times 8$ *k*-point grids were used for solute–solute distances

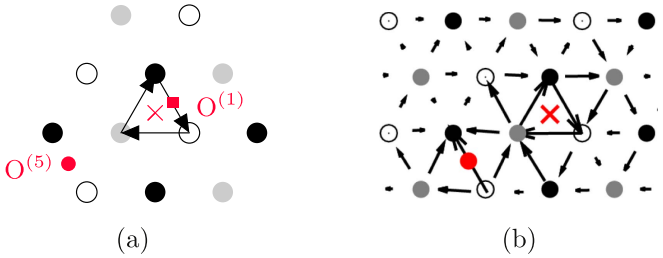

Figure 1. (a) Schematic representation of the first and fifth nearest neighbor positions, respectively $O^{(1)}$ (red square) and $O^{(5)}$ (red dot) for a carbon atom in the vicinity of a dislocation core. (b) Differential displacement map of a dislocation decorated by carbon atoms in $O^{(5)}$ sites (red dot). The configuration shown here was obtained in Ta(C) with $d_{CC} = 1b$. In (a) and (b), the dislocation is in an easy core position (red cross). Metal atoms are represented in white, gray and black depending on their altitude along [111] and the arrows represent the relative displacements along [111] between neighboring atomic columns.

Table 1. Energy difference (in eV) between tetrahedral and octahedral carbon positions in BCC transition metals.

	V	Nb	Ta	Mo	W	Fe
ΔE_{t-o}	1.16	1.34	1.52	1.28	1.51	0.86

of $1b$ and $2b$ respectively. A simulation cell contains a single dipole and these cell dimensions are large enough to yield converged dislocation core energies (Clouet *et al* 2009).

Calculations for interstitial solutes in bulk crystals without dislocation were performed in a 250-atom simulation cell and a $4 \times 4 \times 4$ k-point grid. The preferential position for carbon solutes in group 5 and 6 bulk BCC metals is, as in α-Fe, the octahedral site (see table 1) as reported in previous works (Nguyen-Manh 2008, Ventelon *et al* 2013).

Dislocation dipoles were initially relaxed in pure metals in their easy core configuration, which is the minimum-energy stable configuration in all pure BCC metals. We then introduced either just one carbon atom in an octahedral position in the vicinity of one of the dislocations or two carbon atoms, one next to each dislocation of the dipole. Several octahedral sites close to the dislocation core were investigated. The results presented below focus on the first and fifth nearest neighbor sites, denoted respectively $O^{(1)}$ as in Ventelon *et al* (2015) and $O^{(5)}$ (see figure 1(a)). The systems were then relaxed again to determine whether a spontaneous rearrangement occurred or not (Ventelon *et al* 2015).

The interaction energy per solute atom between the dislocation and the solute atom, E_{int}, is defined as:

$$E_{\text{int}} = E_d - E_\infty, \tag{1}$$

where E_d is the energy when a solute is located near the dislocation and E_∞ is when the solute is infinitely separated from the dislocation. Thus, negative energies correspond to attractive interactions. E_d and E_∞ are computed as:

Table 2. Energy difference (in meV/b) between hard and easy core configurations, noted $\Delta E_{\text{hard}-\text{easy}}$, in BCC transition metals.

	V	Nb	Ta	Mo	W	Fe
VASP (this work)	40	62	39	88	136	40
PWSCF (Dezerald *et al* 2014)	53	76	44	88	129	33

$$E_d = \frac{1}{2}E_{\text{dislo}+C} + E_{\text{bulk}} \text{ and } E_\infty = \frac{1}{2}E_{\text{dislo}} + E_C. \tag{2}$$

$E_{\text{dislo}+C}$ (respectively E_{dislo}) is the energy of a cell containing a dislocation dipole with (respectively without) a solute atom in the vicinity of each core. E_C (respectively E_{bulk}) is the energy of a perfect BCC cell with (respectively without) a solute atom in its most stable position. The factors $\frac{1}{2}$ in E_d and E_∞ are needed when two solutes are introduced, one near each dislocation of the dipole. These factors are omitted when only one solute is introduced.

For the $O^{(1)}$ position, the same configuration is obtained whether one or two carbon atoms are introduced and the interaction energies per solute atom are identical. This shows that the distance between dislocations is large enough to avoid mutual interactions between $\langle 111 \rangle$ arrays of solutes and between a solute on one dislocation and the other dislocation. For the $O^{(5)}$ position on the other hand, we observed that when two carbon atoms are introduced, different configurations may be obtained on each dislocations after relaxation. We have thus introduced in this case a single carbon atom near only one dislocation and we have kept the configuration with the strongest interaction energy.

As will be shown below, the interaction between carbon atoms along $\langle 111 \rangle$ in the bulk is limited to first neighbors. We have checked that the same is true along a reconstructed dislocation in Fe(C) (Ventelon *et al* 2015). In this case, comparing the solute–dislocation interaction energies for solute separations of $1b$ (denoted $E_{\text{int}}(1b)$) and $2b$ (denoted $E_{\text{int}}(2b)$) allows to extract V_{CC}, the first-neighbor solute–solute interaction energy along the dislocation line:

$$V_{CC} = E_{\text{int}}(1b) - E_{\text{int}}(2b) + \Delta E_{\text{hard}-\text{easy}}, \tag{3}$$

where $\Delta E_{\text{hard}-\text{easy}}$ is the cost to transform an easy core of one Burgers vector into a hard core. In case of a core reconstruction as in Fe(C), the contribution $\Delta E_{\text{hard}-\text{easy}}$ must be added since V_{CC} involves a dislocation in its hard core configuration, whereas the dislocation–solute interaction energy is calculated with respect to the easy core. When no core reconstruction occurs, this term is not taken into account. The DFT values for $\Delta E_{\text{hard}-\text{easy}}$ are reported in table 2. They are in good agreement with previous DFT calculations performed with the PWSCF DFT code (Dezerald *et al* 2014).

In the following, V_{CC} will be compared to the interaction energy between solute atoms in the bulk, with the solute atoms placed in octahedral sites and separated by either $1b$ or $2b$ along the $\langle 111 \rangle$ direction. These interaction energies, denoted $V_{CC}^{\text{bulk}}(d_{CC})$ with $d_{CC} = 1b$ or $2b$, are calculated as:

$$V_{CC}^{\text{bulk}}(d_{CC}) = E_{2C}(d_{CC}) + E_{\text{bulk}} - 2E_C, \tag{4}$$

where $E_{2C}(d_{CC})$ is the energy of a perfect BCC cell with two solute atoms in octahedral sites separated by a distance d_{CC} along $\langle 111 \rangle$. From equations (3) and (4), a negative value for V_{CC} and V_{CC}^{bulk} means an attraction between the solute atoms.

Stoichiometric carbide calculations were performed for cubic NaCl- and hexagonal WC-type structures with 2-atom cells and $16 \times 16 \times 16$ k-point grids. The cell volume was

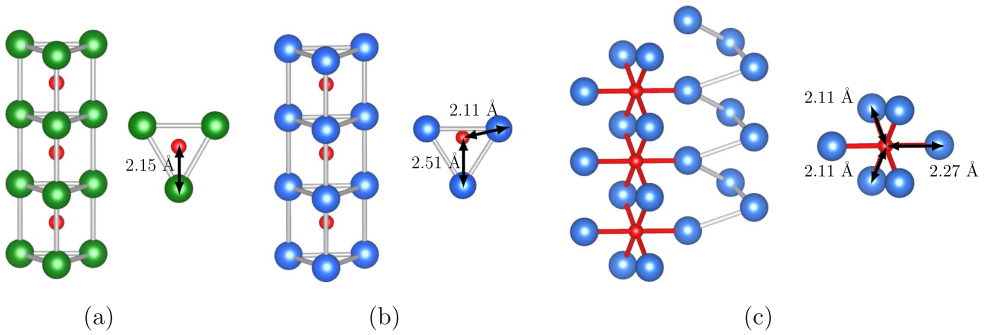

Figure 2. (a), (b) Relaxed structures of the reconstructed dislocation core in the presence of carbon atoms (in red) for (a) group 6 metals (metal core atoms in green) and (b) group 5 metals (metal core atoms in blue). (c) Relaxed structure in Ta(C) of the configuration where the carbon atom is placed in the $O^{(5)}$ position and the dislocation remains in its easy core configuration. M–C distances are reported (in Angströms) in the case of W(C) and Ta(C), and carbon atoms are separated by $1b$ along the Burgers vector direction.

allowed to relax to optimize the lattice parameters a and c (when applicable). The calculations were done for group 4, 5, 6, 7 and 8 transition metals. For all metals, pseudopotentials with p-semicore electrons were used, except for Fe for which a pseudopotential with only valence electrons was used, and Zr for which the pseudopotential includes s- and p-semicore electrons (the p-semicore electron pseudopotential is not currently available in VASP).

3. Carbon–dislocation interaction

3.1. M6(C) systems

In Mo and W, when a carbon atom is placed initially in an $O^{(1)}$ position in the vicinity of the dislocation core, the system is unstable and relaxes towards the same prismatic configuration as in Fe(X) (X = B, C, N and O) (Ventelon *et al* 2015, Lüthi *et al* 2016) for both $d_{CC} = 1b$ and $2b$. The relaxation results in the stabilization of the dislocation hard core around regular trigonal prisms centered on carbon atoms (figure 2(a)). We will refer to these structures as P_{1b} and P_{2b}, respectively. The DFT results of the dislocation–solute interaction energies are presented in figures 3(a) and (b). A strong attraction is found with interaction energies ranging from -1.4 eV to -1.9 eV per solute atom, for both carbon separations of $1b$ and $2b$ along the dislocation line. In order to compare between metals, the interaction energies can be normalized by $k_B T_m$ where T_m is the melting temperature of the metal. Compared to the values in Fe(C), these normalized interaction energies in W(C) and Mo(C) are 60% larger in absolute value for $d_{CC} = 1b$ and similar, within 10%, for $d_{CC} = 2b$. The discrepancy for $d_{CC} = 1b$ reflects the striking difference in the C–C interactions along the dislocation line (see below).

In Fe(C), the same reconstruction occurs when a carbon atom is placed in the octahedral sites at second, third and fourth nearest neighbor distances. On the other hand, the $O^{(5)}$ site is metastable, i.e. upon relaxation, the carbon atom stays in the octahedral site and the dislocation remains in its easy core position but with an energy higher than the reconstructed core (Lüthi *et al* 2016). This configuration is referred to as $O^{(5)}_{1b}$ or $O^{(5)}_{2b}$ depending on the distance between carbon atoms. In Mo and W, the $O^{(5)}$ configuration (figure 1(b)) is also locally stable. The carbon–dislocation interaction energy is attractive, (figures 3(a) and (b)),

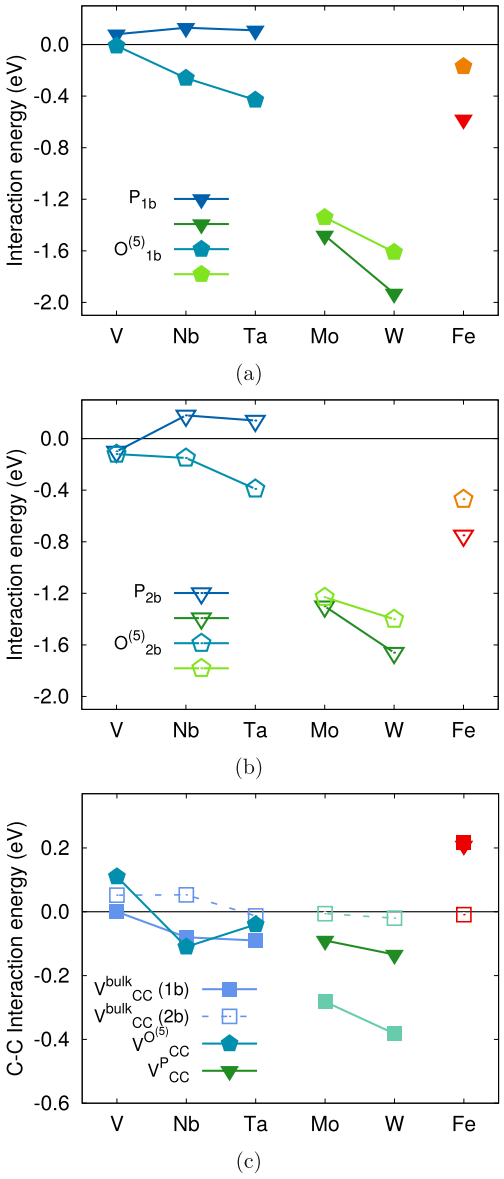

Figure 3. Interaction energies in M(C) systems. (a), (b) Dislocation-carbon interaction energy (in eV per solute atom) in the prismatic and $O^{(5)}$ configurations for two C–C distances: (a) 1b and (b) 2b. (c) Interaction energy between carbon atoms (in eV) along the $\langle 111 \rangle$ direction when they are introduced in octahedral interstitial sites of the bulk BCC crystal, and in the most stable core configuration: the $O^{(5)}$ configuration for group 5 and the prismatic configuration for group 6 and Fe.

but less than for the prismatic configuration ($E_{\text{int}}^{O^{(5)}}(1b) = -1.34$ eV per solute atom for Mo and -1.64 eV per solute atom for W). We thus focus on the prismatic configuration in the following.

C–C interactions are first computed along the dislocation line in the prismatic configuration using equation (3). They are attractive in Mo and W, respectively −0.09 eV and −0.12 eV (figure 3(c)). This contrasts with Fe where the C–C interaction is repulsive (Ventelon *et al* 2015, Lüthi *et al* 2016). This result is however consistent with the C–C interaction energies found in the bulk and also shown in figure 3(c). These energies at a distance of 1*b* along ⟨111⟩ ($V_{CC}^{\text{bulk}} = -0.28$ eV and −0.38 eV respectively) are even more attractive in Mo and W than along the dislocation line, while the same interaction is repulsive in Fe. We also note that at a distance of 2*b*, the bulk C–C interactions are negligible in all metals, which shows, as announced above, that C–C interactions are limited to first neighbors along ⟨111⟩ in the bulk. In conclusion, the qualitative correlation between the interactions in the bulk and along the dislocation is common to all three metals.

3.2. *M5(C) systems*

In *M5*(C) systems (*M5* = V, Nb and Ta), the $O^{(1)}$ octahedral configuration for the carbon atom in the vicinity of the dislocation core is also unstable and relaxes towards the prismatic configuration. However, the carbon atoms are slightly offset from the center of the prisms, as shown in figure 2(c). Moreover, the fifth nearest neighbor position for the carbon atom (position $O^{(5)}$ in figure 1(a)) is found stable and of lower energy than the prismatic configuration. As shown in figure 1(b), no core reconstruction occurs and the dislocation stays in its easy core configuration. Calculations performed in Ta(C) show that the $O^{(2)}$ configuration decays to $O^{(5)}$ and that the $O^{(3)}$ and $O^{(4)}$ sites are locally stable, but with an energy higher than $O^{(5)}$.

The DFT results presented in figures 3(a) and (b) show that in group 5 metals there is a weak carbon–dislocation interaction in the prismatic configuration, with values ranging from −0.1 to 0.1 eV per solute atom, for both carbon separation distances of 1*b* and 2*b* along the dislocation line. The interaction energy for the $O^{(5)}$ configuration is slightly more negative and varies from −0.01 to −0.4 eV per solute atom. In the case of Nb and Ta, the $O^{(5)}$ configuration is more favorable than the prismatic configuration, whereas for V, the energies of both configurations are similar.

The C–C interaction was also investigated along the dislocation line for the prismatic and $O^{(5)}$ configurations (for clarity, the results are represented only for $O^{(5)}$ in figure 3(c)). The interaction is of the same sign as in bulk and slightly attractive, except for V where there is a slight repulsion in both the dislocation core (+0.14 eV) and in the $O^{(5)}$ position (+0.11 eV).

4. Discussion

4.1. *Lattice distorsion energy*

The stability of the carbon atoms in the prismatic sites may arise from a chemical or an elastic effect. One should however be aware that (1) these sites are located at the center of the dislocation, where elasticity doesnt apply; and (2) these sites are highly symmetric and have the same coordination number as bulk interstitial sites.

In order to investigate the origin of the stability of the prismatic configuration, the isolated octahedral configuration in a BCC lattice is compared to the P_{2b} configuration where the prismatic sites can be considered isolated due to their 2*b*-separation. First, Voronoi volumes of solute atoms were calculated for both configurations. The Voronoi volume for the isolated octahedral site is smaller than for the prismatic site by 14.5% before relaxation and by 6% after relaxation (see table 3). This suggests that the matrix deforms more and therefore

Table 3. Unrelaxed and relaxed Voronoi volumes (in Å^3) for a solute at an octahedral position in the bulk and in the P_{2b} configuration. The Voronoi volumes for the $O_{2b}^{(5)}$ configurations are presented for group 5 metals only.

		V	Nb	Ta	Mo	W
Octa.	Unrelaxed	6.74	9.16	9.14	7.89	8.08
	Relaxed	8.13	10.47	10.26	9.27	9.46
P_{2b}	Unrelaxed	7.76	10.57	10.55	9.12	9.33
	Relaxed	8.52	11.23	11.31	9.87	10.07
Difference (in %)	Unrelaxed	14.1	14.3	14.3	14.5	14.4
	Relaxed	4.7	7.0	9.7	6.3	6.2
$O_{2b}^{(5)}$	Unrelaxed	6.77	9.21	9.22		
	Relaxed	7.84	10.29	10.11		
Difference (in %)	Unrelaxed	0.4	0.5	0.9		
	Relaxed	3.6	1.7	1.5		

Table 4. Lattice distortion energies (in eV) for a carbon atom placed in a bulk octahedral configuration, denoted E_{dist}^{O}, and the prismatic configuration with solute separation distance of $2b$, denoted $E_{\text{dist}}^{P_{2b}}$. The carbon–dislocation interaction energy can be estimated by adding the difference between the lattice distortion energies of these two sites, denoted $\Delta E_{\text{dist}}^{P_{2b}-O}$, and twice the energy difference per Burgers vector between the easy and the hard core, $\Delta E_{\text{hard}-\text{easy}}$. This calculation is compared to the interaction energy $E_{\text{int}}(2b)$ as plotted in figure 3(b).

	V	Nb	Ta	Mo	W
E_{dist}^{O}	+0.84	+0.94	+1.04	+1.58	+1.85
$E_{\text{dist}}^{P_{2b}}$	+0.52	+0.41	+0.38	+0.14	+0.36
$\Delta E_{\text{dist}}^{P_{2b}-O} + 2\Delta E_{\text{hard}-\text{easy}}$	−0.24	−0.53	−0.57	−1.26	−1.22
$E_{\text{int}}(2b)$	−0.10	+0.18	+0.14	−1.30	−1.66
$E_{\text{dist}}^{O_{2b}^{(5)}}$	+0.57	+0.57	+0.50		
$\Delta E_{\text{dist}}^{O_{2b}^{(5)}-O}$	−0.27	−0.37	−0.54		
$E_{\text{int}}^{O^{(5)}}(2b)$	−0.12	−0.15	−0.37		

stores more strain energy around an octahedral site than around a prismatic site. The same result was obtained in Fe(X) (Lüthi *et al* 2016).

This strain effect can be estimated using the lattice distorsion energy, which is defined as the energy difference between two systems without solutes (Barouh *et al* 2014, Lüthi *et al* 2016). The reference energy is that of the relaxed system without solute (perfect crystal or hard core) and the energy of the distorted lattice is calculated after removing the solute atom from the relaxed insertion site without further relaxation. The results are presented in table 4. As expected from the Voronoi volumes, in all metals the lattice distortion energy is larger for the octahedral than the prismatic site, as in Fe, but with an even larger amplitude in Mo and W. Therefore, the octahedral site induces a larger deformation than the prismatic site.

Changes in chemical bonds between the carbon and metal atoms and between the metal atoms themselves is at the origin of the stability of the carbon atom in different environments. The energy difference between the bulk and prismatic configurations has different

contributions, mainly a chemical contribution from the bond energies and a strain energy from the lattice distorsion around the carbon atoms. If we neglect the change in metal-carbon bonds between the two sites, the carbon–dislocation interaction energy can be estimated by adding the difference between the lattice distorsion energies in prismatic and octahedral sites plus a correction term $2\Delta E_{\mathrm{hard-easy}}$ due to the core reconstruction. The result is shown in table 4. Similar values are obtained in Mo and W and they compare well with the direct DFT calculation of $E_{\mathrm{int}}(2b)$. This tends to show that, although the strong carbon-metal chemical bonds is at the origin of the high stability of both the octahedral and prismatic sites, the energy difference between these two sites arises primarily from the strain energy and not the chemical energy. However, in the case of W(C), there is still a part of the DFT interaction energy (0.44 eV per solute atom), which remains unexplained by the strain effect and probably corresponds to the change in bond energy between the octahedral and prismatic sites.

In the case of group 5 metals, the structures of the prismatic P_{2b} and $O^{(5)}$ configurations were compared to the bulk octahedral configuration. The Voronoi volume analysis, summarized in table 3, shows that the prismatic configuration is the largest insertion site for the carbon atom. The octahedral $O^{(5)}$ site is also affected by the dislocation as it relaxes less than the bulk octahedral site, although this configuration is the most attractive for the carbon solute. This suggests that the strain effect is not dominant in group 5 metals. This is confirmed by the lattice distorsion energies computed for the isolated octahedral site and the $O^{(5)}$ and prismatic configurations. For $O^{(5)}$, the reference state was chosen as the dislocation easy core. The results are also reported in table 4. The bulk octahedral site is the most distorted insertion site and the interaction energy calculated from the lattice distorsion energy is attractive (between -0.2 eV and -0.6 eV depending on the metal) for both the prismatic and $O^{(5)}$ configurations. This disagrees with the direct DFT calculations (figure 3(b)), which find that the prismatic configuration is slightly repulsive, except for V. For the $O^{(5)}$ configuration, the interaction energies given by the lattice distorsion and DFT are both attractive but $E_{\mathrm{dist}}^{O_{2b}^{(5)-O}}$ is twice $E_{\mathrm{int}}^{O^{(5)}}(2b)$. This indicates that the distorsion energy accounts for a larger part of the interaction energy in the $O^{(5)}$ configuration than in the P_{2b} configuration, but in these metals the strain energy is clearly not sufficient to explain the stability of the considered structures.

4.2. Carbide structures and their link with carbon–dislocation energetics

Group 5 and 6 BCC metals are known to form carbides with different structures: stoichiometric carbides have a cubic NaCl-type structure in group 5 and a hexagonal WC-type structure in group 6. In these structures, carbon atoms are placed at the centers of respectively regular octahedra and regular prisms formed by the six nearest neighbor metal atoms (Hume-Rothery *et al* 1969, Goldschmidt 1967, Toth 1971, Wijeyesekera and Hoffmann 1984, Liu *et al* 1988, Price and Cooper 1989, Hugosson *et al* 1999, Zhong *et al* 2016), see figure 4. This group dependent behavior correlates well with the present results on site preference for carbon atoms at dislocation cores, with the lowest energy for octahedral sites, namely $O^{(5)}$, in group 5, and for prismatic sites in group 6. In this section, the relative stability between both carbide structures is investigated using DFT calculations. For this study, we expanded the investigated metals to groups 4, 7 and 8 in order to obtain a broader view of carbide stability.

In the NaCl-type structure, the carbon atoms can be viewed as occupying all the octahedral sites of the FCC metal lattice, leaving the tetrahedral sites empty, whereas in the WC-type structure, the metal atoms are on a simple hexagonal lattice with a c/a ratio close to 1, and the carbon atoms occupy every other trigonal prismatic site. The occupied prisms are on

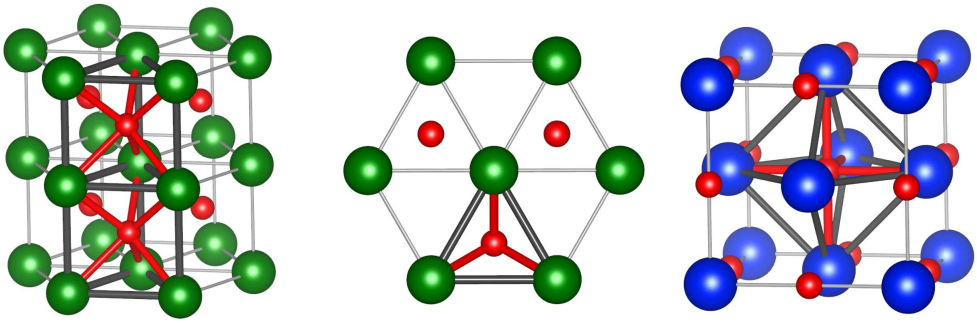

Figure 4. (a), (b) Hexagonal WC-type carbide structure. Metal atoms are represented in green and carbon atoms in red. (a) Visualization in perspective. Two prismatic sites are emphasized by gray metal-metal bonds and red metal-carbon bonds. (b) Projection in the basal plane. (c) Cubic NaCl-type carbide structure. Metal atoms are in blue and carbon atoms in red. One octahedral site is emphasized by gray metal-metal bonds and red metal-carbon bonds.

Table 5. Equilibrium lattice parameters (in Å) for NaCl- and WC-type carbide structures for all non-magnetic transition metals of groups 5 and 6. The values are compared to experimental data (Goldschmidt 1967). The composition of the experimental compound is given in parenthesis when provided (Goldschmidt 1967).

		V	Nb	Ta	Mo	W
NaCl-type	a_0	4.15	4.50	4.47	4.36	4.38
Exp.	a_0	4.17 ($VC_{0.87}$)	4.47 ($NbC_{0.99}$)	4.46 ($TaC_{0.99}$)		
WC-type	a_0	2.83	3.07	3.05	2.91	2.92
	c_0	2.66	2.89	2.88	2.82	2.85
Exp.	a_0				2.90	2.91
	c_0				2.81	2.84

top of each other, sharing faces in the same way as core prisms share ⟨111⟩ faces in the reconstructed dislocation core.

In agreement with literature (Goldschmidt 1967, Hume-Rothery *et al* 1969, Toth 1971, Wijeyesekera and Hoffmann 1984, Liu *et al* 1988, Price and Cooper 1989, Hugosson *et al* 1999, Zhong *et al* 2016), the NaCl structure is found within DFT to be more stable for groups 4 and 5, whereas it is the WC structure for groups 6, 7 and 8. The calculated lattice parameters for both structures in all non-magnetic group 5 and 6 metals are listed in table 5 and are in good agreement with experimental data (Goldschmidt 1967). The metal-carbon distances for these metals are reported in table 6 for both carbide structures and for a bulk octahedral site as well as for the prismatic and $O^{(5)}$ dislocation sites. It can be noticed that the distances are similar in both carbide structures, and close to the distances in the prims and for the second nearest neighbors in the bulk and in the $O^{(5)}$ octahedral interstitial site. Concerning the energy difference between the two carbide structures, as illustrated in figure 5, the same trend is observed for the 3d, 4d and 5d series, with an amplitude increasing slightly from the 3d to the 5d series. Note that a similar trend was obtained by Wijeyesekera and Hoffmann

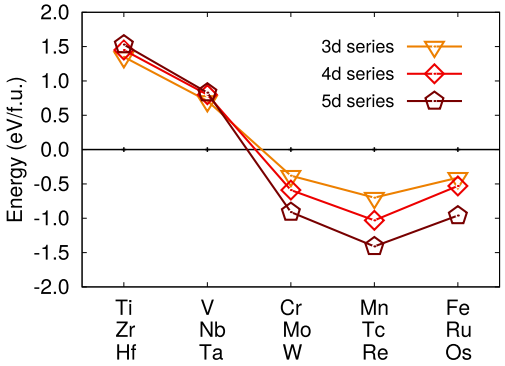

Figure 5. Energy difference in eV per formula unit (f.u.) between hexagonal- and NaCl-type carbide structures. A positive value means that the NaCl-type structure is favored.

Table 6. M–C distances (in Å) for all non-magnetic BCC transition metals from group 5 and 6 for both carbide structures, for the octahedral position in the bulk for the stable 1*b* prism configuration in Mo and W and for the stable $O^{(5)}$ position in V, Nb and Ta. For the octahedral and $O^{(5)}$ configurations, both first and second nearest neighbor metal atoms (1st NN and 2nd NN respectively) are considered.

	V	Nb	Ta	Mo	W
NaCl-type	2.08	2.25	2.24	2.18	2.19
WC-type	2.11	2.28	2.27	2.20	2.21
Octa 1st NN	1.93	2.08	2.06	1.96	1.95
Octa 2nd NN	2.05	2.24	2.23	2.18	2.20
Prism				2.14	2.15
$O^{(5)}$ 1st NN	1.95	2.12	2.11		
$O^{(5)}$ 2nd NN	2.09	2.29	2.27		

(Wijeyesekera and Hoffmann 1984) on the 5d series using an extended Hückel tight binding method.

The calculations on carbide stability are therefore fully consistent with the dislocation calculations: in group 6 metals, regular trigonal prisms—formed in the hexagonal WC structure and in the dislocation hard core—are most stable, while in group 5 metals, the octahedral environment—formed in the cubic NaCl structure and in the $O^{(5)}$ dislocation configuration—is most stable.

5. Summary and conclusions

In the present paper, the interaction between $1/2\langle 111\rangle$ screw dislocations and interstitial carbon atoms was investigated in all non-magnetic BCC transition metals (group 5: V, Nb and Ta; group 6: Mo and W). The DFT calculations show that in group 6 metals, carbon solute atoms can stabilize the hard core configuration with the solutes placed at the center of trigonal prisms formed by the metal atoms inside the three $\langle 111\rangle$ atomic columns of the hard core, as reported previously in Fe(X) (X = B, C, N, O). The solute–dislocation interaction energy is strongly attractive, ranging from -1.3 to -1.9 eV per solute atom. A large part of this energy is attributed, in the case of a 2*b* solute–solute distance along the dislocation line, to the local

distorsion of the matrix. In group 5 metals, the solute atom is slightly off-centered in the metastable prismatic configuration, while the fifth nearest neighbor octahedral site is the most stable configuration. The dislocation–solute interaction energy is weakly repulsive for the prismatic configuration and attractive for the $O^{(5)}$ configuration but the distorsion energy is not sufficient in this case to explain these interactions. The stability of the core configuration can be linked to the stability of stoichiometric carbides, where WC and MoC adopt a hexagonal WC-type structure, formed by regular trigonal prisms on top of each other, as in the dislocation prismatic core. On the other hand, VC, NbC and TaC take a NaCl-like structure, with an octahedral environment for the carbon atom.

Acknowledgments

This work was performed using GENCI-CINES computer center under Grant No. 2015-096821 and the HELIOS supercomputer system at IFERC, Aomori Japan. DR would like to acknowledge support from LABEX IMUST (ANR-10-LABX-0064) of University of Lyon (programme 'Investissements d'Avenir', ANR-11-IDEX-0007). This work has been carried out within the framework of the EUROfusion Consortium and has received funding from the Euratom research and training programme 2014–2018 under Grant Agreement No. 633053. The views and opinions expressed herein do not reflect those of the European Commission.

References

Barouh C, Schuler T, Fu C C and Nastar M 2014 *Phys. Rev.* B **90** 054112
Blöchl P E 1994 *Phys. Rev.* B **50** 17953
Chockalingam K, Janisch R and Hartmaier A 2014 *Modelling Simul. Mater. Sci. Eng.* **22** 075007
Clouet E, Ventelon L and Willaime F 2009 *Phys. Rev. Lett.* **102** 055502
Cottrell A H and Bilby B A 1949 *Proc. Phys. Soc.* A **62** 49
Dezerald L, Ventelon L, Clouet E, Denoual C, Rodney D and Willaime F 2014 *Phys. Rev.* B **89** 024104
Goldschmidt H J 1967 *Intersitial Alloys* (London: Butterworths)
Hugosson H W, Eriksson O, Nordtröm L, Jansson U, Fast L, Delin A, Wills J M and Johansson B 1999 *J. Appl. Phys.* **86** 3758
Hume-Rothery W, Smallman R E and Haworth C W 1969 *The Structure of Metals and Alloys* (London: The Metal and Metallurgy Trust)
Ishii A, Li J and Ogata S 2013 *PLoS One* **8** e60586
Itakura M, Kaburaki H, Yamaguchi M and Okita T 2013 *Acta Mater.* **61** 6857
Kresse G and Furthmüller J 1996 *Phys. Rev.* B **54** 11169
Kresse G and Joubert D 1999 *Phys. Rev.* B **59** 1758
Li H, Wurster S, Motz C, Romaner L, Ambrosch-Draxl C and Pippan R 2012 *Acta Mater.* **60** 748
Liu A Y, Wentzcovitch R M and Cohen M L 1988 *Phys. Rev.* B **38** 9483–9
Lüthi B, Ventelon L, Rodney D and Willaime F 2016 *Private Communication*
Medvedeva N I, Gornostyrev Y N and Freeman A J 2007 *Phys. Rev.* B **76** 212104
Nguyen-Manh D 2008 *Adv. Mater. Res.* **59** 253
Oyama S T 1996 *The Chemistry of Transition Metal Carbides and Nitrides* (Netherlands: Springer)
Price D L and Cooper R 1989 *Phys. Rev.* B **39** 4945
Rodney D, Ventelon L, Clouet E, Pizzagalli L and Willaime F 2016 *Acta. Mater.* **124** 633–59
Romaner L, Ambrosch-Draxl C and Pippan R 2010 *Phys. Rev. Lett.* **104** 195503
Romaner L, Razumovskiy V I and Pippan R 2014 *Phil. Mag. Lett.* **94** 334
Samolyuk G D, Osetsky Y N and Stoller R E 2013 *J. Phys.: Condens. Matter* **25** 025403
Tapasa K, Osetsky Y N and Bacon D J 2007 *Acta Mater.* **55** 93
Toth L E 1971 *Transition Metal Carbides and Nitrides* (New York: Academic)
Trinkle D R and Woodward C 2005 *Science* **310** 1665
Veiga R G A, Goldenstein H, Perez M and Becquart C S 2015 *Scr. Mater.* **108** 19

Ventelon L, Lüthi B, Clouet E, Proville L, Legrand B, Rodney D and Willaime F 2015 *Phys. Rev.* B **91** 220102(R)
Ventelon L, Willaime F, Clouet E and Rodney D 2013 *Acta Mater.* **61** 3973
Wijeyesekera S D and Hoffmann R 1984 *Organometallics* **3** 949–61
Zhao Y and Lu G 2011 *Modelling. Simul. Mater. Sci. Eng.* **19** 065004
Zhong Y, Xia X, Shi F, Zhan J, Tu J and Fan H J 2016 *Adv. Sci.* **3** 1500286